

# Aspartate-279 in Aminolevulinate Synthase Affects Enzyme Catalysis through Enhancing the Function of the Pyridoxal 5'-Phosphate Cofactor<sup>†</sup>

Jian Gong,<sup>‡,||</sup> Gregory A. Hunter,<sup>‡,||</sup> and Gloria C. Ferreira<sup>\*,‡,§,⊥</sup>

Department of Biochemistry and Molecular Biology, College of Medicine, Institute for Biomolecular Science, and H. Lee Moffitt Cancer Center and Research Institute, University of South Florida, Tampa, Florida 33612

Received August 5, 1997; Revised Manuscript Received December 26, 1997

**ABSTRACT:** 5-Aminolevulinate synthase (ALAS) catalyzes the first step in the heme biosynthetic pathway in nonplant eukaryotes and some prokaryotes, which is the condensation of glycine with succinyl-coenzyme A to yield coenzyme A, carbon dioxide, and 5-aminolevulinate. ALAS requires pyridoxal 5'-phosphate as an essential cofactor and functions as a homodimer. D279 in murine erythroid enzyme was found to be conserved in all aminolevulinate synthases and appeared to be homologous to D222 in aspartate aminotransferase, where the side chain of the residue stabilizes the protonated form of the cofactor ring nitrogen, thus enhancing the electron sink function of the cofactor during enzyme catalysis. D279A mutation in ALAS resulted in no detectable enzymatic activity under standard assay conditions, and the conservative D279E mutation reduced the catalytic efficiency for succinyl-CoA 30-fold. The D279A mutation resulted in a 19-fold increase in the dissociation constant for binding of the pyridoxal 5'-phosphate cofactor. UV-visible and CD spectroscopic analyses indicated that the D279A mutant binds the cofactor in a different mode at the active site. In contrast to the wild-type and D279E mutant, the D279A mutant failed to catalyze the formation of a quinonoid intermediate upon binding of 5-aminolevulinate. Importantly, this partial reaction could be rescued in D279A by reconstitution of the mutant with the cofactor analogue *N*-methyl-PLP. The steady-state kinetic isotope effect when deuteroglycine was substituted for glycine was small for the wild-type enzyme ( $k^H/k^D = 1.2 \pm 0.1$ ), but a strong isotope effect was observed with the D279E mutant ( $k^H/k^D = 7.7 \pm 0.3$ ). pH titration of the external aldimine formed with ALA indicated the D279E mutation increased the apparent  $pK_a$  for quinonoid formation from 8.10 to 8.25. The results are consistent with the proposal that D279 plays a crucial role in aminolevulinate synthase catalysis by enhancing the electron sink function of the cofactor.

5-Aminolevulinate synthase (ALAS)<sup>1</sup> (EC 2.3.1.37) is the first enzyme in the heme biosynthetic pathway in animals, fungi, and some bacteria, and it catalyzes the condensation

of glycine and succinyl-CoA to produce 5-aminolevulinate (ALA), coenzyme A, and carbon dioxide (1, 2). In animals, two chromosomally distinct genes have been identified, one of which appears to be expressed exclusively in erythrocytes (3). The high degree of sequence homology between the two gene products, which are 70% identical for the mature human enzymes, indicates a structural identity and suggests the two isoforms differ primarily in regulation of expression (3). Pyridoxal 5'-phosphate (PLP) is required as an essential cofactor, and a reaction mechanism has been proposed on the basis of radiolabeling studies (4). K313 of murine erythroid ALAS has been identified as the residue involved in the Schiff base linkage with the PLP cofactor (5), and a conserved glycine loop has been proposed to form part of the PLP-binding site (6).

ALAS is a member of the  $\alpha$ -family of PLP-dependent enzymes, in which the covalency changes occur at the  $\alpha$ -carbon of the amino acid that forms an aldimine linkage to the PLP cofactor through the amino group (7, 8). The members of this enzyme family, which include the transaminases, are believed to share a common evolutionary origin (7), and sequence homology analyses have revealed the absolute conservation of an aspartate residue approximately 30–40 residues to the N-terminus of the perfectly conserved lysine that forms the Schiff base linkage with the

<sup>†</sup> This work was supported by the National Science Foundation (Young Investigator Award MCB-9257656 to G.C.F.), and the National Institutes of Health (Grant DK52053 to G.C.F.). J.G. and G.A.H. are recipients of Predoctoral Fellowships from the American Heart Association, Florida Division (93GSF/9 to J.G. and 9504006 to G.A.H.). G.A.H. was also the recipient of a Summer Research Assistantship in 1995 from the Institute of Biomolecular Science at the University of South Florida.

\* Author to whom correspondence should be addressed. Telephone: (813) 974-5797. Fax: (813) 974-5798. E-mail: gferreir@com1.med.usf.edu.

<sup>‡</sup> Department of Biochemistry and Molecular Biology, College of Medicine.

<sup>§</sup> Institute for Biomolecular Science.

<sup>||</sup> Co-first authors.

<sup>⊥</sup> H. Lee Moffitt Cancer Center and Research Institute.

<sup>1</sup> Abbreviations: ALA, 5-aminolevulinate; ALAS, 5-aminolevulinate synthase; PLP, pyridoxal 5'-phosphate; AAT, aspartate aminotransferase; TPL, tyrosine phenol-lyase; DGD, dialkylglycine decarboxylase; TAT, tyrosine aminotransferase; HPAT, histidinol-phosphate aminotransferase; ACCS, 1-aminocyclopropane-1-carboxylate synthase; GAT, glycine C-acetyltransferase; AOS, 8-amino-7-oxononanoate synthase; EDTA, ethylenediaminetetraacetate; SDS, sodium dodecyl sulfate; SDS-PAGE, SDS-polyacrylamide gel electrophoresis; BSA, bovine serum albumin; AMPPO, [3-(1,1-dimethyl-2-hydroxyethyl)-amino]-2-hydroxypropanesulfonic acid; CD, circular dichroism; KIE, C- $\alpha$ -kinetic isotope effect.

cofactor (7, 9). Significantly, in the  $\alpha$ -family enzymes for which three-dimensional structures are available, including AAT (10), TPL (11), and DGD (12, 13), this aspartate residue is positioned to interact with the pyridinium ring nitrogen of the PLP cofactor. The negatively charged carboxylate group of the aspartate residue appears to be spatially situated to play a critical role in stabilizing the protonated form of the ring nitrogen, thus enhancing the electron sink character of the cofactor during catalysis. In AAT, mutation of the conserved aspartate residue (D222) to alanine resulted in an 8600-fold decrease in the catalytic efficiency, and even a conservative change to glutamate reduced activity 4-fold (14). Significantly, the D222A and D222N mutations increased the deuterium isotope effect with  $[2\text{-}^2\text{H}]$  aspartate from 2.2 to 6.0, indicating that these mutations do impair the efficiency with which the PLP cofactor functions as an electron sink. Reconstitution of the D222A mutant with *N*-methyl-PLP, a cofactor analogue where the ring nitrogen has a permanent positive charge, led to a 10-fold recovery of enzymatic activity, even though crystallographic studies indicated that the cofactor analogue was not positioned in an optimal orientation at the active site (15). In murine erythroid ALAS the corresponding aspartate residue is D279, and to test if this residue enhances the electron sink character of the PLP cofactor in a manner analogous to AAT, we have used site-directed mutagenesis to replace D279 by alanine or glutamate. The results provide further evidence to support the postulated role of this conserved residue in catalysis by the  $\alpha$ -family of PLP-dependent enzymes.

## EXPERIMENTAL PROCEDURES

### Materials

Restriction enzymes, Vent DNA polymerase, and T<sub>4</sub> DNA ligase were obtained from New England Biolabs, and were used according to the manufacturer's instructions. Sequenase and deoxy- and dideoxynucleotide triphosphates were from Amersham.  $[\alpha\text{-}^{35}\text{S}]$  dATP was from Du Pont/NEN Research Products. The bicinchoninic acid protein assay reagents were purchased from Pierce Chemical Co. All other chemicals were purchased from Sigma or Fisher and were of the highest purity available. The oligonucleotide primers were synthesized in the DNA Synthesis Core Laboratory (University of Florida). The GeneClean II kit was a product of Bio 101 Inc., while the QIAquick PCR Purification kit and QIAGEN-tip 100 Plasmid DNA Preparation kit were from Qiagen. Ultrogel AcA 44 was obtained from IBF Biotechnics Inc. HiTrap desalting columns were from Pharmacia Biotech. Acrylamide and gel reagents were purchased from Bio-Rad. Dialysis tubing was obtained from Spectrum Medical Industries. Centricon concentrators and Amicon ultrafiltration cells and membranes were obtained from Amicon.

### Methods

**Comparison of Conserved Residues in ALAS and Some Related PLP-Dependent Enzymes.** Protein sequences were retrieved via computer from the public database at the National Center for Biotechnology Information (NCBI). The sequences for each enzyme were aligned using the program CLUSTAL to identify conserved residues for that enzyme. Conserved residues comprising the active site of AATase

(the enzyme most closely related to ALAS for which a crystal structure is known) were then used as markers to visually look for conservation of similar residues in ALAS and some other related enzymes, using the active site lysine that forms a Schiff base with the PLP cofactor as a reference point. This procedure for identifying putative active site residues is similar to that previously described for ACCS (16).

**Construction of Plasmids pJG8 and pJG15.** The pJG8 and pJG15 plasmids encode the full length sequence for the mature murine erythroid ALAS D279A and D279E mutants, respectively, and are derived from the pJG3 plasmid encoding the sequence for the mature murine erythroid ALAS (6). The method for constructing both plasmids was based on the method described by Chen and Przybyla (17), with some modifications. Briefly, two rounds of PCR were performed to obtain DNA fragments with the desired mutation flanked by two unique restriction enzyme digestion sites. The DNA fragments were then amplified by a third round of PCR, digested with the two unique restriction endonucleases, and subcloned back into the pJG3 vector. The first round of PCR generated DNA products that encoded either the D279A or the D279E mutation and contained a unique *Sma*I restriction site, a unique restriction enzyme site downstream of the mutation. The mutagenic primer for D279A was 5'-CTTCGTAGCTGAAGTCCA, where the nucleotide substitution introduced is underlined, and for D279E was 5'-CTTCGTA(G/A)ANGAAGTCCA, where (G/A) = 50% G + 50% A, and N = 25% each of G, A, T, and C. The downstream primer used was 5'-TTGAGTAGGCGCACAGA. The PCR mixture (100  $\mu$ L) contained 25 ng of the pJG3 DNA as the template, 50 pmol of each primer, 200  $\mu$ M dideoxynucleotide triphosphates, 1 unit of Vent DNA polymerase, and reaction buffer (New England Biolabs). A total of 25 cycles of 94 °C for 1 min, 45 °C for 3 min, and 72 °C for 2 min was followed by an extension of 10 min at 72 °C. The PCR products were purified using the QIAquick PCR purification kit (Qiagen). The purified products were then used as megaprimers for the second round of PCR, which generated DNA fragments with the desired mutation flanked by the *Sma*I site and a unique *Xho*I site upstream of the mutation region. The reaction mixture for the second round of PCR (200  $\mu$ L) contained 300 ng of the megaprimer, 50 pmol of the upstream primer, 5'-CATAAGCAGACACCTAGGGT, and the remaining components in the same amounts as used in the first round of PCR described above. The program was also the same as that for the first round of PCR. The generated product was gel purified, and 50 ng was used as the template for a third round of PCR, using the upstream and downstream primers. The amounts of other reaction components and the program were the same as those in the first round of PCR. The resulting PCR products were purified, using the QIAquick PCR purification kit. The purified DNA fragments were digested with *Sma*I and *Xho*I, and subcloned into the pJG3 vector, which had been previously digested with the same endonucleases. DNA sequencing was performed according to the dideoxynucleotide chain-termination method (18) to verify the mutations.

**Protein Purification, SDS-PAGE, and Protein Determinations.** Wild-type and mutant forms of ALAS were purified from bacterial extracts containing the overexpressed protein as previously described (19). Buffer A (20 mM potassium phosphate, pH 7.2, containing 1 mM EDTA, 5 mM  $\beta$ -mer-

captoethanol, 10% glycerol, and 20  $\mu\text{M}$  PLP) was used throughout the purification and the subsequent characterization experiments unless otherwise stated. Protein purity was estimated by SDS-PAGE (20) and was never less than 95%. Protein concentrations were determined by the bicinchoninic acid assay using BSA as standard, following Pierce's Application Note #13 as the protocol. Briefly, 50  $\mu\text{L}$  of each protein sample was precipitated with 200  $\mu\text{L}$  of ice-cold acetone and then resuspended in 50  $\mu\text{L}$  of deionized water. Subsequently, 1 mL of the BCA working reagent was added to each sample. A blank was prepared by adding 1 mL of the BCA working reagent to 50  $\mu\text{L}$  of deionized water. After incubation at 37 °C for 30 min, the absorbance of each sample was recorded at 562 nm, using the blank as reference. Bovine serum albumin was used as the standard and was treated in a manner identical to the samples.

**Steady-State Kinetics.** Steady-state activity of ALAS was measured at 30 °C by coupling the production of coenzyme A to the reduction of  $\text{NAD}^+$  by  $\alpha$ -ketoglutarate dehydrogenase and monitoring the increase in absorbance at 340 nm (21). The assay conditions were 20 mM HEPES, pH 7.2, 1 mM  $\text{NAD}^+$ , 3 mM  $\text{MgCl}_2$ , 250  $\mu\text{M}$  thiamine pyrophosphate, 0.25 unit of  $\alpha$ -ketoglutarate dehydrogenase, 5–200 mM glycine, 1–30  $\mu\text{M}$  succinyl-coenzyme A, and 2.7  $\mu\text{M}$  (wild-type) or 6.1  $\mu\text{M}$  (D279E) ALAS. Data were constructed as matrixes of five glycine and five succinyl-CoA concentrations from which apparent maximal velocities were determined by fitting the data to the Michaelis–Menten equation using the nonlinear regression analysis software program *Enzfitter* (Biosoft Publishing Inc.). Data were collected in duplicate for both enzymes. Secondary plots were used to obtain  $K_m$  and  $k_{\text{cat}}$  values as described (22).

**Dissociation Constants for Glycine and ALA.** Equilibrium dissociation constants for the binding of glycine to the wild-type and mutant proteins were determined at pH 7.5 and 30 °C by separately titrating the proteins (20  $\mu\text{M}$  for each protein) with increasing concentrations of glycine and monitoring the increase in absorbance at 420 nm upon formation of the external aldimine between PLP and glycine (19). Binding of ALA to the wild-type enzyme or D279E ALAS resulted in a decrease in absorbance at 420 nm, and instead there was a new absorption maximum formed at 510 nm (wild-type ALAS), or 500 nm (D279E ALAS), indicating the formation of a quinonoid intermediate. Thus, for binding of ALA to the wild-type and D279E mutant the absorbance increase of the quinonoid was used to calculate the  $K_d$  values. Conversion of the external aldimine to a quinonoid intermediate upon ALA binding was not observed for the D279A mutant, however, and the  $K_d$  for this interaction was calculated from the increase in absorbance at 420 nm. In all cases the data were analyzed by nonlinear regression analysis to determine the  $K_d$  as previously described (23).

**Chemical Synthesis and Purification of *N*-Methyl-PLP.** *N*-Methyl-PLP was synthesized by methylation of the free base form of PLP with a molar equivalence of dimethyl sulfate, as described by Pfeuffer et al. (24). The cofactor analogue was purified from unreacted starting material by traditional column anion exchange chromatography at pH 8.5 using 0.1 M sodium bicarbonate as loading buffer and 0.25 M sodium bicarbonate for elution.

**Preparation of Apo-ALAS Enzymes and Reconstitution of D279A ALAS with *N*-Methyl-PLP.** Apoenzymes of both the

wild-type and the D279A mutant forms were obtained through extensive dialysis at 4 °C against buffer A minus PLP. The enzymes were dialyzed against at least 10 times enzyme sample volumes of buffer A, with multiple changes of the buffer throughout the dialysis. Activity assays and/or UV–visible spectral analyses were performed to monitor the dialysis process, since it has been reported that apo-ALAS is inactive and does not exhibit the 420 nm absorbance maximum corresponding to the Schiff base formed between the enzyme and the cofactor (19). The apo-ALAS preparations were concentrated to the desired final concentration using centricon-30 concentrators or Amicon ultrafiltration cells with a YM30 or YM10 membrane.

To obtain the D279A ALAS reconstituted with *N*-methyl-PLP, apo D279A was treated with a 10-fold molar excess of *N*-methyl-PLP for 1 h at 25 °C, and then the excess analogue was removed by overnight dialysis, after which the reconstituted protein was concentrated as described above. Immediately before use, 1.5 mL of concentrated sample was applied to a HiTrap desalting column (16 mm  $\times$  25 mm, Pharmacia Biotech) to separate any free cofactor analogue from the holoenzyme. The sample was eluted with 5 mL of buffer A without PLP. Spectra of the eluted fractions were recorded, and the fractions containing the reconstituted holoenzyme were collected and pooled.

**Spectroscopic Methods: UV–Visible and CD Spectra.** Absorption spectra were recorded using a Shimadzu UV 2100U dual-beam spectrophotometer at 25 °C. ALAS wild-type and mutant samples (10–20  $\mu\text{M}$ ) were dialyzed for 6 h against three changes of buffer A containing PLP or *N*-methyl-PLP at a concentration 110% of that of the enzyme. The dialyzed samples were centrifuged to remove any denatured protein. The absorption spectra were then recorded using the dialysate as reference.

CD spectra were obtained using a Jasco J710 spectropolarimeter calibrated for both wavelength maxima and signal intensity using an aqueous solution of D-10-camphorsulfonic acid (25). UV spectra (2–10  $\mu\text{M}$  enzyme) were recorded over the wavelength range 200–270 nm using a cylindrical cell of 0.1 cm path length and a total volume of 300  $\mu\text{L}$ . Visible CD spectra obtained during apoenzyme titrations (8–15  $\mu\text{M}$  enzyme) with PLP or *N*-methyl-PLP were recorded using a cylindrical cell of 1 cm path length and a total volume of 600  $\mu\text{L}$ . All spectra were obtained at 25 °C and are corrected for buffer contributions.

**Determination of  $K_d$ , the Equilibrium Constant for Dissociation of PLP or *N*-Methyl-PLP from ALAS.**  $K_d$  values were determined by CD spectrometric titration of the apo ALAS enzyme with PLP or *N*-methyl-PLP. ALAS wild-type and the D279A mutant form were in buffer A minus PLP at a concentration range of 8–15  $\mu\text{M}$ . A series of PLP or *N*-methyl-PLP stocks were prepared, and a minimal volume of each was added to the enzyme cuvette to achieve the desired PLP or *N*-methyl-PLP concentration, such that the total dilution of the protein sample was less than 5% and could be assumed to be insignificant. CD spectra in the 400–500 nm region were recorded after each addition of PLP or *N*-methyl-PLP. The changes in the spectra were used to calculate the  $K_d$  values.  $K_d$  is defined as

$$K_d = [\text{ALAS}]_{\text{apo}}[\text{C}]_{\text{ub}}/[\text{ALAS}]_{\text{holo}} \quad (1)$$

where  $[\text{ALAS}]_{\text{apo}}$  and  $[\text{C}]_{\text{ub}}$  are concentrations of the apo ALAS and unbound PLP or *N*-methyl-PLP, respectively, and  $[\text{ALAS}]_{\text{holo}}$  represents the concentration of the holo ALAS. The ratio  $R$  of bound PLP (or *N*-methyl-PLP) to total PLP- (or *N*-methyl-PLP) was derived as

$$R = (1/2)\{1 + K_d/[\text{C}]_t + [\text{ALAS}]_t/[\text{C}]_t - [(1 + K_d/[\text{C}]_t + [\text{ALAS}]_t/[\text{C}]_t)^2 - 4[\text{ALAS}]_t/[\text{C}]_t]^{1/2}\} \quad (2)$$

where  $[\text{C}]_t$  is the total PLP or *N*-methyl-PLP concentration and  $[\text{ALAS}]_t$  is the total ALAS concentration.

Changes in the apparent ellipticities at 420 nm (or 440 nm for D279A) were plotted against  $[\text{C}]_t$ , and the  $K_d$  was determined by fitting the data to eq 2 using the nonlinear regression analysis program *Enzfitter*.

**Detection of the Quinonoid Intermediate in ALAS-Catalyzed Reverse Reaction.** The quinonoid intermediate was detected from the ALAS-catalyzed reverse reaction by monitoring the absorbance in the 400–600 nm range at 25 °C. Four hundred microliters of ALAS in buffer A (4–5  $\mu\text{M}$  for the wild-type enzyme and 40–80  $\mu\text{M}$  for D279A mutant ALAS) was mixed with 40  $\mu\text{L}$  of 0.5 M AMPSO buffer, pH 9. Two hundred microliters of this mixture was subsequently transferred into both the sample and the reference cuvettes. The reaction was started by the addition of 10  $\mu\text{L}$  of 0.5 M ALA-hydrochloride in water freshly neutralized with 10  $\mu\text{L}$  of 0.5 M KOH, while 20  $\mu\text{L}$  of water was added to the reference. The absorbance in the range of 400–600 nm was recorded immediately after the sample was mixed. The appearance of an absorbance maximum at 510 nm reflected formation of the quinonoid reaction intermediate.

**Kinetic Isotope Effect with D279E.** Enzyme activity was monitored continuously at 30 °C using a coupled enzyme assay essentially as described (21) with either 100 mM glycine or 100 mM deuteroglycine, 50  $\mu\text{M}$  succinyl-CoA, and 8.3  $\mu\text{M}$  wild-type ALAS or 15  $\mu\text{M}$  D279E ALAS. Each set of conditions was run three times, and the values reported represent the average value with the standard error of measurement.

**pH Titration of Quinonoid Formation with D279E.** To examine the possible pH dependence of quinonoid formation with ALA, a pH gradient was created by titrating a 60  $\mu\text{L}$  solution of 1 M HEPES free acid or 1 M AMPSO free acid with increasing volumes of 1 M sodium hydroxide. Following the mixing of buffer and sodium hydroxide, 12  $\mu\text{L}$  of a 1 M solution of ALA-hydrochloride was added to the buffer, followed by a volume of water sufficient to bring the total volume up to 500  $\mu\text{L}$ . After mixing this solution with a handheld pipet, 100  $\mu\text{L}$  of 120  $\mu\text{M}$  D279E ALAS was added to yield a final solution containing 100 mM buffer of varying pH, 20 mM ALA, and 20  $\mu\text{M}$  D279E. Twenty millimolar ALA was determined to be sufficient to saturate the D279E mutant over the pH range 6.5–9.3 in control experiments. The solution was thoroughly mixed in the sample cuvette, and the spectrum was immediately recorded from 250 to 600 nm. Following the spectral scan, the pH of the solution was checked by diluting the sample 2-fold with water in a scintillation vial and reading the pH on a Fisher Scientific Accumet 915 pH meter. The dilution was necessary to achieve a sufficient volume of liquid to make

an accurate reading possible, and it had no effect on the final pH as determined in separate control experiments. HEPES was used as buffer in the pH range 6.5–8.2, and AMPSO was used in the pH range 8.2–9.4. The blank solution in the reference cell was a solution of 100 mM of the appropriate buffer in the free acid form and 10 mM ALA-hydrochloride. It was essential to keep the blank acidic because at neutral to basic pH values there was a time-dependent increase in absorbance throughout the observed wavelength range, with the increase being much more pronounced at shorter wavelengths. This was presumably caused by some degree of polymerization of the ALA, which is an aminoketone, at pH values where a significant portion of the molecules were present as the free amine, since this effect was not observed in the absence of ALA or when the pH of the solution was below 7.0. To avoid any effects this might have on the measured quinonoid formation the reference solution was allowed to remain acidic, and the spectrum of the sample solution was recorded immediately after mixing the enzyme into the solution. The absorbance at 510 nm as a function of pH was fitted to the equation

$$\text{Abs} = [(\text{Abs}_{\text{max}} - \text{Abs}_{\text{min}})/(1 + 10^{(\text{pK} - \text{pH}))}] + \text{Abs}_{\text{min}} \quad (3)$$

while the absorbance at 420 nm was fitted to the equation

$$\text{Abs} = [(\text{Abs}_{\text{max}} - \text{Abs}_{\text{min}})/(1 + 10^{(\text{pH} - \text{pK}))}] + \text{Abs}_{\text{min}} \quad (4)$$

using the nonlinear regression analysis program *Enzfitter*, where  $\text{Abs}_{\text{max}}$  and  $\text{Abs}_{\text{min}}$  represent the theoretical maximal and minimal absorbance at 510 nm under the defined conditions, respectively, and along with the  $\text{pK}$  term are the variables in the equation.

## RESULTS

**Comparison of Conserved Residues in ALAS and Some Related PLP-Dependent Enzymes.** The three-dimensional structure of ALAS is currently unknown, but sequence, secondary structure prediction, and hydrophobicity profile analyses indicate a significant structural similarity to several other PLP-dependent enzymes, including transaminases (7, 9). In support of these computational analyses, crystallographic studies have shown that the PLP binding domains of AATase, DGD, and TPL are similar (11, 13). Several of the residues comprising the active site are conserved, and even more strikingly, their spacing within the peptide sequence relative to the active site lysine that forms a Schiff base to the cofactor is also conserved. A comprehensive model postulating the roles of these residues in catalysis by AAT has been published (10), and subsequent mutagenic studies have supported this model (14, 15, 27–30). We have found that many of these active site residues are also perfectly conserved in the 20 known ALAS sequences, as well as in glycine acetyltransferase and 8-amino-7-oxononanoate synthase, and postulate they may exhibit functions analogous to those of the corresponding residues in AAT (Figure 1).

Among these conserved amino acids the aspartate residue which is approximately 30–40 amino acids to the N-terminus of the lysine involved in Schiff base linkage with PLP is of particular interest. In AAT, TPL, and DGD, this residue is

A.

	70	194	195	197	222	225	255	258	266	268	386						
AAT (n=29) — Y	NP	-	G	-	D	-	Y	-	S <sup>a</sup>	K	-	R	-	G	-	R	
	-188	-64-63	-61	-36	-33	-3	0	+8	+10							+128	
TPL (n=6) — Y	N	-	G	-	D	-	R	-	S	-	K					R	
	-186	-72	-69	-43	-40	-3	0									+124	
DGD (n=1) —				G	-	D	-	Q	-	T	-	K				R	
				-56	-29	-26	-3	0								+134	
TAT (n=6) — Y	NP	-	G	-	D	-	Y	-	K	-	R	-	G	-	R		
	-171	-63-62	-60	-35	-32			0	+8	+10	+128						
HPAT (n=18) — Y <sup>b</sup>	NP	-	G	-	D	-	Y	-	T	-	K	-	R	-	G	-	R
	-175	-55-54	-52	-29	-26	-3	0	+8	+10	+129							
ACCS (n=23) — Y	NP	-	G	-	D	-	Y <sup>c</sup>	-	S <sup>d</sup>	-	K	-	R <sup>e</sup>	-	G	-	R <sup>f</sup>
	-186	-69-68	-66	-41	-38	-3	0	+8	+10	+134							
ALAS (n=20) — Y	SM	-	G	-	D	-	H	-	T	-	K					R	
	-192	-59-58	-56	-34	-31	-3	0									+128	
GAT (n=2) — Y	SM	-	G	-	D	-	H	-	T	-	K					R	
	-190	-59-58	-56	-34	-31	-3	0									+131	
AOS (n=11) — Y	SM <sup>g</sup>	-	G <sup>h</sup>	-	D	-	H	-	T	-	K					R	
	-190	-59-58	-56	-34	-31	-3	0									+126	

B.

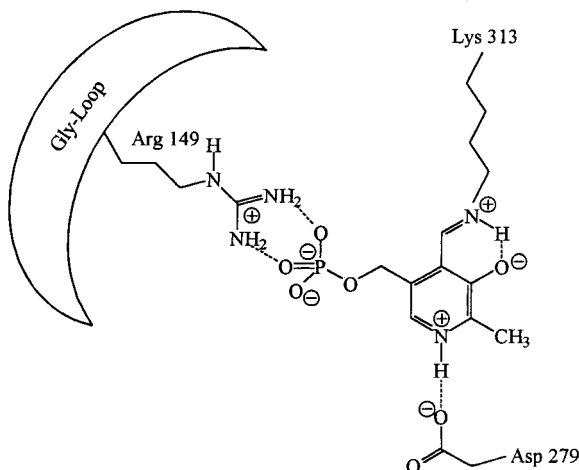


FIGURE 1: (A) Conserved residues in ALAS and some  $\alpha$ -family PLP-enzymes. Numberings used for enzymes are the following: chicken cytosolic AAT (9), *Citrobacter freundii* TPL (10); *Pseudomonas cepacia* DGD (37); *Escherichia coli* TAT (38); *Saccharomyces cerevisiae* HPAT (39), apple ACCS (40), mouse erythroid ALAS (41), *E. coli* GAT (7), and *Bacillus sphaericus* AOS (7). Numbers below each residue indicate their distance (in terms of numbers of residues) from the Schiff base lysine residue (positive numbers are designated to be C-terminal to the lysine, while negative numbers mean the residues are N-terminus to the lysine). The number of sequences aligned for each enzyme is given adjacent to the enzyme name: <sup>a</sup>glycine in *Archae* and some eubacteria; <sup>b</sup>serine in *Rhizobium* sp.; <sup>c</sup>phenylalanine in wheat; <sup>d</sup>glycine in wheat; <sup>e</sup>glycine in geranium; <sup>f</sup>serine in leaf mustard; <sup>g</sup>alanine in mycobacteria; <sup>h</sup>alanine in *Helicobacter pylori*. (B) Model for the partial active site of ALAS. Residue numbering is for the murine erythroid ALAS (41).

located within a distance of strong ionic interaction with the ring nitrogen of PLP. The negatively charged side-chain carboxylate group of this residue plays a critical role in stabilizing the protonated ring nitrogen of the cofactor, which enables PLP to function as an electron sink during enzyme catalysis (14, 15). In mouse erythroid ALAS, D279 appears to be the residue homologous to D222 in AAT, according to the sequence comparison (Figure 1).

**Kinetic Analysis and Dissociation Constants.** The steady-state kinetics of wild-type and D279E were examined, and the results are presented in Table 1. Double reciprocal crossover plots of the raw data indicated a sequential mechanism. The conservative mutation decreased the  $k_{\text{cat}}$  approximately 2-fold and decreased the catalytic efficiency

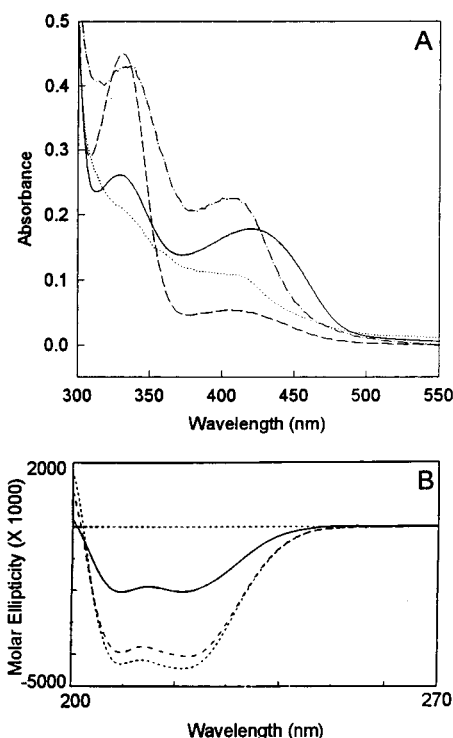


FIGURE 2: (A) Absorption spectra of wild-type and mutant ALASs. (—), Wild-type at 18.2  $\mu\text{M}$ ; (···) D279A in PLP form at 18.8  $\mu\text{M}$ , (---), D279A reconstituted with *N*-methyl-PLP at 19.3  $\mu\text{M}$ , (- · - ·), D279E at 19.0  $\mu\text{M}$ . Spectra were recorded in 20 mM potassium phosphate buffer, pH 7.2, in a 1 cm cell, as described in Experimental Procedures. (B) CD spectra of ALAS wild-type and D279A mutant enzymes. (—) Wild-type ALAS at 10  $\mu\text{M}$ , (---) D279A in PLP form at 6  $\mu\text{M}$ , (···) D279A in *N*-methyl-PLP form at 8  $\mu\text{M}$ .

for glycine 10-fold. The catalytic efficiency for succinyl-CoA was decreased 30-fold. Since the D279A mutation resulted in an activity below the detection limit, D279A was subsequently reconstituted with *N*-methyl-PLP and assayed for activity. *N*-Methyl-PLP is a PLP analogue, which has a methyl group linked to the ring nitrogen. The ring nitrogen is therefore permanently positively charged, and this might circumvent the need for the aspartate residue. However, reconstitution with the cofactor analogue did not rescue enzymatic activity to a measurable extent under the standard assay conditions (data not shown).

The enzymes were titrated with glycine and ALA to determine the dissociation constants for formation of external aldimines with substrate and product. Mutation of D279 to glutamate or alanine increased the  $K_d$  for glycine about 3.5-fold. More interesting results were observed for binding of the product, ALA, where the D279E mutation increased the  $K_d$  64-fold and the D279A mutation increased the  $K_d$  400-fold.

**Absorption and CD Spectroscopic Characterization of ALAS.** Figure 2A compares the visible absorption spectra of wild-type ALAS with the D279E mutant, and the D279A mutant in either the PLP or *N*-methyl-PLP forms. For the wild-type ALAS, two absorbance maxima were observed around 330 and 420 nm, respectively. These two absorbance maxima presumably represent different ionization states of the imine nitrogen of the internal aldimine formed between K313 in ALAS and the PLP cofactor. In the D279E mutant the 430 nm absorption was slightly blue-shifted to about 410

Table 1: Steady-State Kinetic and Equilibrium Parameters for Reaction of ALAS

ALAS	$k_{\text{cat}}$ ( $\text{min}^{-1}$ )	glycine			SCoA		ALA
		$K_{\text{m}}$ (mM)	$k_{\text{cat}}/K_{\text{m}}$ ( $\text{min}^{-1} \text{mM}^{-1}$ )	$K_{\text{d}}^a$ (mM)	$K_{\text{m}}$ ( $\mu\text{M}$ )	$k_{\text{cat}}/K_{\text{m}}$ ( $\text{min}^{-1} \mu\text{M}^{-1}$ )	$K_{\text{d}}^b$ (mM)
wild-type	$10 \pm 1$	$23 \pm 1$	$0.4 \pm 0.04$	$22 \pm 2$	$2.3 \pm 0.1$	$4.5 \pm 0.5$	$0.025 \pm 0.003$
D279E	$5.8 \pm 0.8$	$140 \pm 30$	$0.04 \pm 0.01$	$76 \pm 7$	$35 \pm 5$	$0.16 \pm 0.04$	$1.6 \pm 0.1$
D279A	$<0.01$			$81 \pm 6$			$10 \pm 1$

<sup>a</sup> From three replicate spectrophotometric titrations at pH 7.2 in buffer A minus PLP. <sup>b</sup> From three replicate spectrophotometric titrations at pH 8.9 in 50 mM AMPSO buffer containing 10% (v/v) glycerol.

nm, and the ratio of the 330 nm to the 410 nm peak heights was markedly increased. The D279A mutant also displayed an absorbance maximum around 420 nm, although the absorption maximum was lower than the wild-type value. Moreover, the mutant exhibited a poor absorbance maximum around 330 nm. These data suggest that the binding of PLP is affected upon mutation of the aspartate residue. When D279A was reconstituted with *N*-methyl-PLP, two absorbance maxima were detected around 330 and 408 nm, respectively, indicating the enzyme can bind to the cofactor analogue. The shift of the 420 nm absorbance to 408 nm is probably indicative of a difference in the interaction of the protein with PLP and *N*-methyl-PLP.

The CD spectra in the region of 200–270 nm were recorded for wild-type ALAS and D279A in both PLP and *N*-methyl-PLP forms (Figure 2B). There was no significant difference in the spectral pattern, suggesting that no gross conformational change was introduced through the mutation of aspartate residue or the reconstitution of the mutant with cofactor analogue. It is likely, however, as has been proposed with other mutants of PLP-dependent enzymes (30, 31), that small conformational changes would be confined to the region immediately surrounding the site of the mutation.

In contrast, significant differences in the CD spectra were detected between the wild-type and the mutant in both PLP and *N*-methyl-PLP forms in the region of 350–500 nm. The wild-type enzyme exhibited a strong positive band around 420 nm. The mutant in both forms displayed two positive bands, around 410 and 440 nm, with molar ellipticities lower than those of the wild-type enzyme (i.e., ranging from 13 to 30% of the wild-type enzyme values, data not shown); these results suggest that the cofactor binding mode must differ between the wild-type enzyme and the mutant.

**Determination of  $K_{\text{d}}$ , the Affinity Constant for Binding of PLP or *N*-Methyl PLP to D279A ALAS.** To characterize further the effects of mutation of D279 in relation to the PLP cofactor at the ALAS active site, the equilibrium constant for dissociation of PLP or *N*-methyl-PLP was determined for the mutant and compared with the wild-type  $K_{\text{d}}$  value. This was accomplished through CD titration of the apoenzyme with PLP or its analogue in the visible region. Changes in the apparent ellipticity were plotted against PLP or *N*-methyl-PLP concentrations in the sample. The  $K_{\text{d}}$  value was determined from the theoretical curve that best fits the experimental data. The results are illustrated in Figure 3; D279A exhibited less affinity for the PLP cofactor than the wild-type ALAS, as the  $K_{\text{d}}$  value was increased 19-fold from 1.6 to 30  $\mu\text{M}$ . The mutant binds *N*-methyl-PLP even less tightly, as the  $K_{\text{d}}$  value was 42-fold higher than that of the wild-type enzyme with PLP.

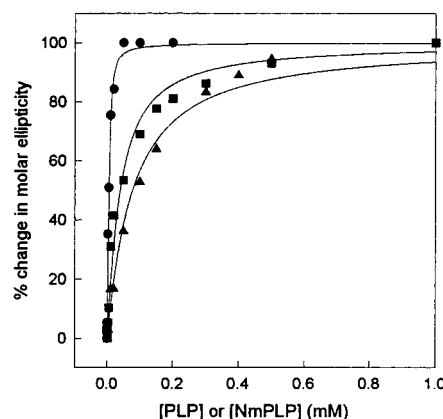


FIGURE 3: CD titration of wild-type and D279A mutant apo-ALAS enzymes with PLP or *N*-methyl-PLP. The titration was performed by recording CD spectra of ALAS enzymes in the presence of 0–1 mM PLP or *N*-methyl-PLP. Changes in the apparent molar ellipticities (at 440 nm for D279A and 420 nm for the wild-type) were plotted as a function of [PLP] or [*N*-methyl-PLP] for each enzyme. (●) Wild-type ALAS (7.1  $\mu\text{M}$ ) titrated with PLP, (■), D279A ALAS (19  $\mu\text{M}$ ) titrated with PLP, (▲) D279A ALAS (19  $\mu\text{M}$ ) titrated with *N*-methyl-PLP. The determined  $K_{\text{d}}$ 's were  $1.6 \pm 0.1 \mu\text{M}$  for wild-type ALAS,  $30 \pm 1 \mu\text{M}$  for D279A, and  $68 \pm 3 \mu\text{M}$  for D279A reconstituted with *N*-methyl-PLP.

**Detection of Quinonoid Intermediate in the Reverse Direction of the Reaction Catalyzed by D279A Reconstituted with *N*-Methyl-PLP.** The D279A mutation rendered the activity of the enzyme to be below the detection limit of the current ALAS activity assay, so any kinetic or isotope effect characterization of this mutant became impracticable. In an effort to elucidate the role of D279 in ALAS catalysis, a partial reaction involving the formation of the quinonoid intermediate in the ALAS-catalyzed reverse reaction was studied. The addition of ALA to the wild-type enzyme leads to the appearance of an absorbance maximum at 510 nm, which results from the formation of a quinonoid intermediate.<sup>2</sup> Not surprisingly, mutation of the aspartate residue abolished the ability of the enzyme to catalyze the production of the intermediate, and as a result, no absorbance maximum was detectable at 510 nm. However, reconstitution of D279A with *N*-methyl-PLP rescued the partial reaction. An absorbance maximum around 510 nm was observed upon addition of ALA to the reconstituted mutant, although the absorption maximum was much lower than that of the wild-type (Figure 4).

**Kinetic Isotope Effect.** To assess the effect of the D279E mutation upon enzymatic removal of the *pro-R* proton of glycine, both the wild-type and D279E mutant were examined for a KIE when deuteroglycine was substituted for

<sup>2</sup> G. A. Hunter and G. C. Ferreira, manuscript in preparation.

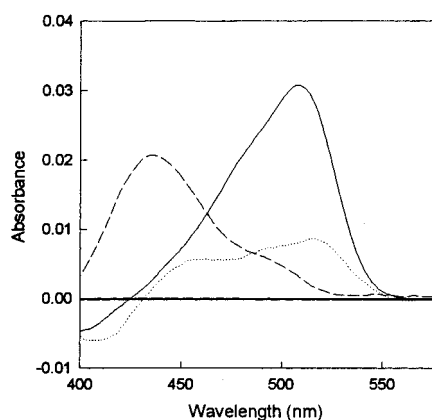


FIGURE 4: A. Detection of the quinonoid intermediate in the wild-type ALAS and D279A-catalyzed reverse reaction. (—) Wild-type ALAS at  $7.4 \mu\text{M}$ , (---) D279A in PLP form at  $50 \mu\text{M}$ , (···) D279A reconstituted with *N*-methyl-PLP at  $48 \mu\text{M}$ . Reactions were performed in  $50 \text{ mM}$  AMPSO buffer, pH 9.0, at  $30^\circ\text{C}$ . ALA-hydrochloride was neutralized with KOH immediately before being added to the enzyme sample. Absorption spectra were recorded upon addition of ALA to  $25 \text{ mM}$ .

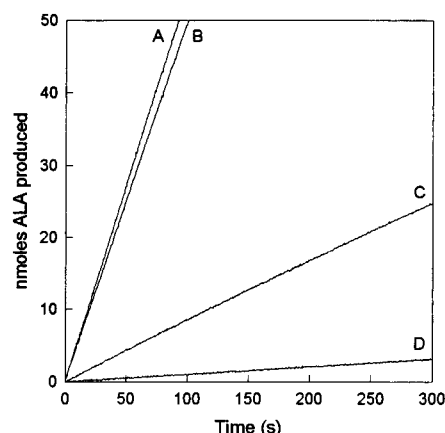


FIGURE 5: Steady-state kinetics of wild-type and D279E ALAS with glycine and deuteroglycine: (A)  $8.3 \mu\text{M}$  wild-type ALAS plus  $100 \text{ mM}$  glycine, (B)  $8.3 \mu\text{M}$  wild-type ALAS plus  $100 \text{ mM}$  deuteroglycine, (C)  $15 \mu\text{M}$  D279E ALAS plus  $100 \text{ mM}$  glycine, (D)  $15 \mu\text{M}$  D279E ALAS plus  $100 \text{ mM}$  deuteroglycine. Each set of conditions was assayed three times, and the lines shown represent the average values for the three runs. For wild-type ALAS  $k^{\text{H}}/k^{\text{D}} = 1.2 \pm 0.1$ , and for D279E ALAS  $k^{\text{H}}/k^{\text{D}} = 7.7 \pm 0.3$ .

glycine during steady-state catalysis. The average time course values of the analyses are shown in Figure 5. The KIE observed for the wild-type enzyme was small but significant ( $1.2 \pm 0.1$ ), indicating that removal of the *pro-R* proton of glycine was only partially rate-limiting. With D279E, however, the KIE was increased to  $7.7 \pm 0.3$ , indicating cleavage of this bond had become entirely rate-limiting with this conservative mutation.

**$pK_a$  for Quinonoid Formation with D279E.** We have observed with the wild-type ALAS that quinonoid formation in the presence of saturating levels of ALA is pH-dependent, with quinonoid formation being favored as the pH is increased. Titration of the ALA saturated wild-type enzyme gave an apparent  $pK_a$  for quinonoid formation of 8.10 with an extinction coefficient for the quinonoid of  $38,300 \text{ M}^{-1} \text{ cm}^{-1}$ .<sup>2</sup> Figure 6A shows the spectra of ALA saturated D279E ALAS at various pH values, and Figure 6B gives the titration results, which indicate the mutation shifts the  $pK_a$  for quinonoid formation with ALA from 8.10 to 8.25.

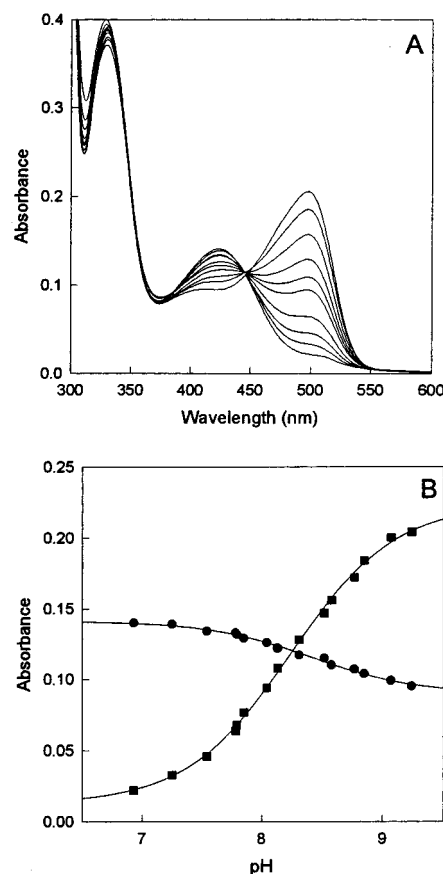


FIGURE 6: (A) UV-vis spectra of  $20 \text{ mM}$  D279E ALAS in the presence of  $20 \text{ mM}$  ALA at various pH values. The pH was (from the lowest to highest absorbing spectrum at  $500 \text{ nm}$ ) 6.92, 7.25, 7.52, 7.78, 8.04, 8.13, 8.31, 8.58, 8.77, and 9.07. (B) Plot of the observed absorbance at  $500 \text{ nm}$  (increasing with pH) and  $425 \text{ nm}$  (decreasing with pH). The curves are the best fit lines as determined by nonlinear regression analysis using eqs 3 and 4, and give a  $pK_a$  of 8.25.

The calculated extinction coefficient for the D279E mutant quinonoid is  $40,620 \text{ M}^{-1} \text{ cm}^{-1}$ . The values for the extinction coefficients of both the ALAS wild-type and D279E quinonoid forms are similar to those estimated for the quinonoid forms produced during the reaction of either serine hydroxymethylase with L-phenylalanine (32, 33) or tryptophanase with alanine (34).

## DISCUSSION

PLP-dependent enzymes that catalyze reactions involving amino acid substrates all utilize the cofactor to facilitate the specific, heterolytic cleavage of one of the bonds to the  $\alpha$ -carbon of the substrate, which is covalently attached to the cofactor via a Schiff base linkage. The electrons from the cleaved bond delocalize into the pyridinium ring and reside primarily on the ring nitrogen, forming a quinonoid intermediate. To act as an electron acceptor and facilitate this process the pyridine ring nitrogen must be protonated, thus enhancing the lability of the bonds to the  $\alpha$ -carbon of the substrate (35). The  $pK_a$  of the pyridine nitrogen of pyridoxal Schiff bases is about 5.9 in aqueous solution (36), so at physiological pH values only a small fraction of the molecules will be in the proper protonation state for catalytic bond cleavage. Members of the  $\alpha$ -family of PLP-dependent enzymes appear to have evolved to create an active site

environment that raises this  $pK_a$  substantially by positioning the side chain carboxylate of an aspartic acid residue within a distance of strong ionic interaction of the PLP ring nitrogen, thus ensuring the proper protonation state for catalysis even at elevated pH values. This aspartate residue resides 30–40 amino acids to the N-terminus of the perfectly conserved lysine residue that forms the Schiff base linkage with the PLP cofactor (Figure 1) (7, 9).

The work reported here investigated the role of D279 in ALAS function. This aspartate residue is conserved in all known ALAS sequences from a variety of sources, and is 34 amino acids N-terminal of the lysine involved in Schiff base linkage with PLP (Figure 1). To define the role of D279 in ALAS function, site-directed mutagenesis was employed to obtain the D279A and D279E mutant enzymes. Replacement with alanine results in the loss of the carboxyl group, while the conservative glutamate mutation displaces the carboxyl group one methylene group farther away from the peptide backbone.

Purified D279A exhibited no detectable activity, even when reconstituted with *N*-methyl-PLP (data not shown). This is not surprising, because the catalytic efficiency for wild-type AAT is over 1000 times that of ALAS, and since the D222A mutation in AAT leads to  $10^4$ -fold decrease in the catalytic efficiency, and reconstitution with *N*-methyl-PLP increases this activity by only 10-fold (13, 14), it can be calculated that similar losses of activity in ALAS would result in activities below the detection limit of the current assay (21). The lack of detectable activity with the D279A mutant indicates that the presence of the carboxyl group of the side chain at this position is crucial to enzyme activity. Additionally, since the conservative D279E mutation decreased the  $k_{cat}$  to approximately 50% of that of the wild-type enzyme, it is also apparent that the spatial positioning of the carboxyl group is important to the integrity of enzyme activity.

The spectroscopic characterization and  $K_d^{PLP}$  determination for D279A provide evidence to implicate D279 in PLP binding (Figures 2 and 3). As the mutation did not introduce any gross change in the overall conformation of the enzyme, the altered binding mode could only suggest that the mutated residue is directly positioned in the cofactor binding pocket. Moreover, D279 contributes considerably to the cofactor binding affinity, as replacement with alanine leads to 19-fold increase in the  $K_d$  value.

The reconstituted mutant exhibits an even lower affinity for the cofactor analogue, reflected in the 42-fold increase in the  $K_d$  value, as compared to that of the wild-type enzyme for PLP (Figure 3). This may explain, at least in part, why the cofactor analogue could not fully rescue the activity of the mutant. In fact, crystallographic studies on D222A AAT reconstituted with *N*-methyl-PLP reveal that the cofactor is not held in a proper orientation within the active site of the enzyme (14). The active site in the mutant AAT undergoes significant rearrangement to accommodate the PLP analogue, and as a result *N*-methyl-PLP is not held in the most favorable position to work as an electron sink during enzyme catalysis (14). In addition, steric hindrance also causes weak binding of the cofactor analogue to the mutant enzyme (14).

If D279 is positioned to protonate the PLP ring nitrogen it would be expected that mutation of this residue would impair the electron-withdrawing capacity of the cofactor. This

would be manifest as a decrease in enzymatic formation of the quinonoid intermediates that form upon addition of glycine plus succinyl-CoA or ALA to the enzyme.<sup>2</sup> We conducted several experiments to test this hypothesis, with the results shown in Figures 4–6. Since ALAS forms a stable quinonoid upon binding ALA alone, we first examined the effect of mutation of D279 upon quinonoid formation with ALA. In contrast to the wild-type enzyme, the D279A mutant yields no absorbance maximum around 510 nm in the presence of ALA (Figure 4), indicating that abstraction of the proton from ALA is severely impaired. Importantly, when the mutant is reconstituted with *N*-methyl-PLP, some accumulation of the quinonoid intermediate is detected at 510 nm. This result suggests that by “fixing” a positive charge at the ring nitrogen position, some electron-withdrawing ability of the cofactor in the mutant is recovered in this partial reaction. A similar approach was not possible for the forward reaction because ALAS does not form an observable quinonoid with glycine alone. A quinonoid intermediate does form upon addition of succinyl-CoA to the ALAS–glycine complex, but this intermediate forms and decays to products too rapidly to measure accurately using conventional spectroscopy.<sup>2</sup>

The electron-withdrawing capacity of the cofactor in the forward reaction was studied using deuteroglycine to look for an isotope effect during cleavage of the *pro-R* C–H bond. When glycine was replaced by deuteroglycine the KIE observed for wild-type ALAS during steady-state enzyme catalysis was very small ( $k^H/k^D = 1.2$ ), indicating that cleavage of the *pro-R* C–H bond of glycine is not rate-limiting for the overall reaction, and instead some other step such as substrate binding or product release is rate-limiting. When D279 was conservatively mutated to glutamate, however, the KIE increased to 7.7, indicating that removal of the *pro-R* proton of glycine had become entirely rate-limiting for the overall reaction. The appearance of a steady-state KIE with deuteroglycine when D279 is mutated to glutamate demonstrates that this mutation *specifically* impairs the ability of the enzyme to utilize the cofactor as an effective electron sink and cleave the *pro-R* proton bond of glycine; other steps in the reaction sequence are not so adversely affected.

Spectrophotometric titration of the ALA saturated D279E mutant showed that the apparent  $pK_a$  for quinonoid formation was raised from 8.10 to 8.25 by the mutation. This result shows that the mutation results in a lessened ability of the enzyme to use the PLP cofactor as an electron sink to form the quinonoid intermediate at physiological pH. One possible explanation for this is that the side chain carboxyl group has been displaced by the mutation and thus does not stabilize the protonated form of the cofactor ring nitrogen as effectively. Alternatively, it could also be argued that the  $pK_a$  of the side chain of glutamate, which at 4.5 is higher than that of aspartate (4.1), raises the apparent  $pK_a$  for quinonoid formation. In either case, the results indicate D279 plays a role in enhancing the function of PLP as an electron sink.

Taken together, the work described here is consistent with the proposal that D279 in ALAS contributes to the proton abstraction that occurs during ALAS catalysis by stabilizing the protonated PLP ring nitrogen. Figure 1B summarizes the current knowledge about the PLP cofactor binding pocket in ALAS. K313 forms a Schiff base linkage to the aldehyde



group of the cofactor (5); a conserved glycine-rich loop motif containing a catalytically essential arginine residue anchors the phosphate group of PLP (6), and finally, D279 interacts electrostatically with the ring nitrogen of the cofactor.

## ACKNOWLEDGMENT

We recognize Dr. Jack F. Kirsch at the University of California at Berkeley for suggesting the homology modeling of ALAS with other PLP-dependent enzymes. The assistance of Dr. Michael J. Barber in conducting the CD analyses is acknowledged. Finally, we thank Drs. R. Franco, P. Gunaratne, M. Leverone, A. Pereira, and P. Tavares and Mr. D. Tan for suggestions on this project and for critical reading of the manuscript.

## REFERENCES

1. Ferreira, G. C., and Gong, J. (1995) *J. Bioenerg. Biomembr.* 27, 151–159.
2. Jordan, P. M. (1991) in *Biosynthesis of Tetrapyrroles* (Jordan, P. M., Ed.) pp 1–66, Elsevier, Amsterdam, The Netherlands.
3. Riddle, R. D., Yamamoto, M., and Engel, J. E. (1989) *Proc. Natl. Acad. Sci. U.S.A.* 86, 792–796.
4. Ahktar, M., and Jordan, P. M. (1979) *Comprehensive Organic Chemistry*, Vol. 5, pp 1121–1144, Pergamon Press, New York.
5. Ferreira, G. C., Neame, P. J., and Dailey, H. A. (1993) *Protein Sci.* 2, 1959–1965.
6. Gong, J., and Ferreira, G. C. (1995) *Biochemistry* 34, 1678–1685.
7. Alexander, F. W., Sandmeier, E., Mehta, P. K., and Christen, P. (1994) *Eur. J. Biochem.* 219, 953–960.
8. John, R. A. (1995) *Biochim. Biophys. Acta* 1248, 81–96.
9. Grishin, N. V., Phillips, M. A., and Goldsmith, E. J. (1995) *Protein Sci.* 4, 1291–1304.
10. Kirsch, J. F., Eichele, G., Ford, G. C., Vincent, M. G., and Jansonius, J. N. (1984) *J. Mol. Biol.* 174, 497–525.
11. Antson, A. A., Demidkina, T. V., Gollnick, P., Dauter, Z., Von Tersch, R. L., Long, J., Berezhnoy, S. N., Phillips, R. S., Harutyunyan, E. H., and Wilson, K. S. (1993) *Biochemistry* 32, 4195–4206.
12. Toney, M. D., Hohenester, E., Cowan, S. W., and Jansonius, J. N. (1993) *Science* 261, 756–759.
13. Toney, M. D., Hohenester, E., Keller, J. W., and Jansonius, J. N. (1995) *J. Mol. Biol.* 245, 151–179.
14. Yano, T., Kuramitsu, S., Tanase, S., Morino, Y., and Kagamiyama, H. (1992) *Biochemistry* 31, 5878–5887.
15. Yano, T., Hinoue, Y., Chen, V. J., Metzler, D. E., Miyahara, I., Hirotsu, K., and Kagamiyama, H. (1993) *J. Mol. Biol.* 234, 1218–1229.
16. White, M. F., Vasquez, J., Yang, S. F., and Kirsch, J. F. (1994) *Proc. Natl. Acad. Sci. U.S.A.* 91, 12428–12432.
17. Chen, B., and Przybyla, A. E. (1994) *BioTechniques* 17, 657–659.
18. Sanger, F., Nicklen, S., and Coulson, A. R. (1977) *Proc. Natl. Acad. Sci. U.S.A.* 74, 5463–5467.
19. Ferreira, G. C., and Dailey, H. A. (1993) *J. Biol. Chem.* 268, 584–590.
20. Laemmli, U. K. (1970) *Nature* 227, 680–685.
21. Hunter, G. A., and Ferreira, G. C. (1995) *Anal. Biochem.* 226, 221–224.
22. Cornish-Bowden, A. (1979) in *Fundamentals of Enzyme Kinetics*, pp 110–112, Butterworths, Boston.
23. Wang, Z., Kumar, N. R., and Srivastava, D. K. (1992) *Anal. Biochem.* 206, 376–381.
24. Pfeuffer, T., Ehrlich, J., and Helmreich, E. (1972) *Biochemistry* 11, 2125–2136.
25. Chen, G. C., and Yang, J. T. (1977) *Anal. Lett.* 10, 1195–1207.
26. Toney, M. D., and Kirsch, J. F. (1993) *Biochemistry* 32, 1471–1479.
27. Inoue, K., Kuramitsu, S., Okamoto, A., Hirotsu, K., Higuchi, T., Morino, Y., and Kagamiyama, H. (1991) *J. Biochem.* 109, 570–576.
28. Toney, M. D., and Kirsch, J. F. (1991) *Biochemistry* 30, 7456–7461.
29. Danishefsky, A. T., Onnufer, J. J., Petsko, G. A., and Ringe, D. (1991) *Biochemistry* 30, 1980–1985.
30. Smith, D. L., Almo, S. C., Toney, M. D., and Ringe, D. (1989) *Biochemistry* 28, 8166–8167.
31. Ferreira, G. C., Vajapey, U., Hafez, O., Hunter, G. A., and Barber, M. J. (1995) *Protein Sci.* 4, 1001–1006.
32. Ulevitch, R. J., and Kallen, R. G. (1977) *Biochemistry* 16, 5350–5354.
33. Ulevitch, R. J., and Kallen, R. G. (1977) *Biochemistry* 16, 5355–5361.
34. Metzler, C. M., Viswanath, R., and Metzler, D. E. (1991) *J. Biol. Chem.* 266, 9374–9381.
35. Metzler, D. E., Longenecker, J. B., and Snell, E. E. (1954) *J. Am. Chem. Soc.* 76, 639–644.
36. Metzler, D. E. (1957) *J. Am. Chem. Soc.* 79, 485.
37. Keller, J. W., Baurick, K. B., Rutt, G. C., O'Malley, M. V., Sonafank, N. L., Reynolds, R. A., Ebbesson, L. O. E., and Vajdos, F. F. (1990) *J. Biol. Chem.* 265, 5531–5539.
38. Fotheringham, I. G., Dacey, S. A., Taylor, P. P., Smith, T. J., Hunter, M. G., Finlay, M. E., Primrose, S. B., Parker, D. M., and Edwards, R. M. (1986) *Biochem. J.* 234, 593–604.
39. Nishiwaki, K., Hayashi, N., Irie, S., Chung, D.-H., Harashima, S., and Oshim, Y. (1987) *Mol. Gen. Genet.* 208, 159–167.
40. Dong, J. G., Kim, W. T., Yip, W. K., Thompson, G. A., Li, L., Bennett, A. B., and Yang, S. F. (1991) *Planta* 185, 38–45.
41. Schoenhaut, D. S., and Curtis, P. J. (1986) *Gene (Amsterdam)* 48, 55–63.

BI9719298